CHAPTER 5

RESULTS & DISCUSSION

5.1 Results

5.1.1 First case: Dehydration of natural gas by zeolite molecular sieves

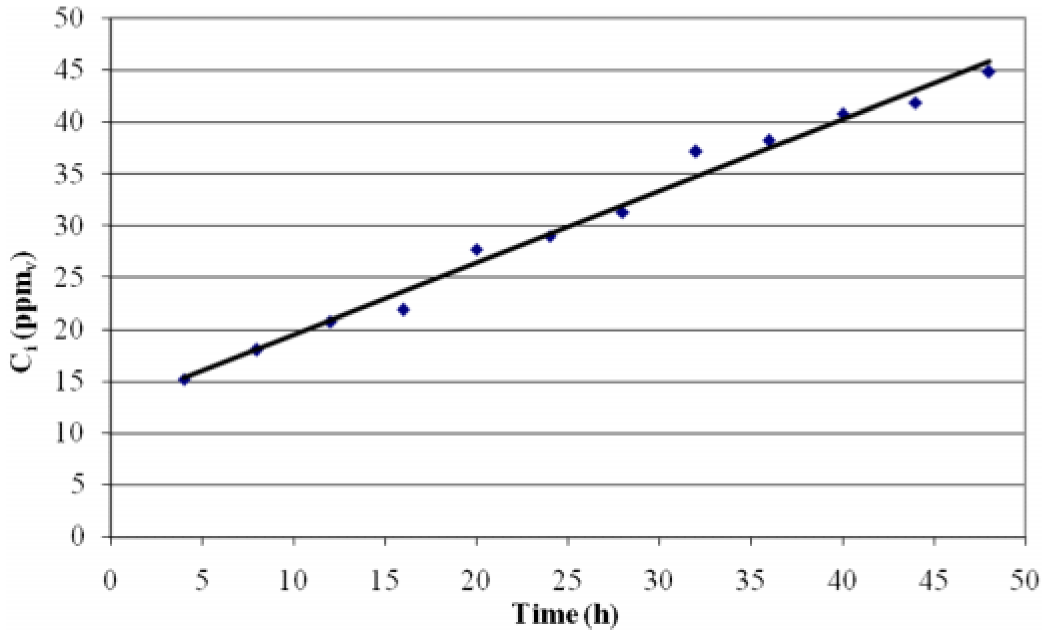

Figure 5.1 Variations of measured inlet concentrations of water vapor in natural gas with time (batch 1: Adsorption step)

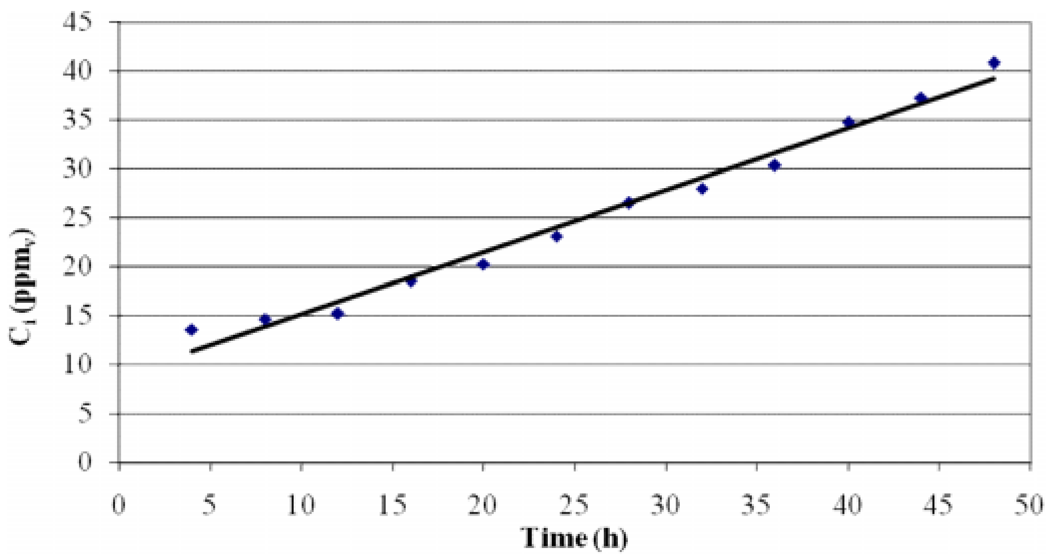

Figure 5.2. Variations of measured inlet content

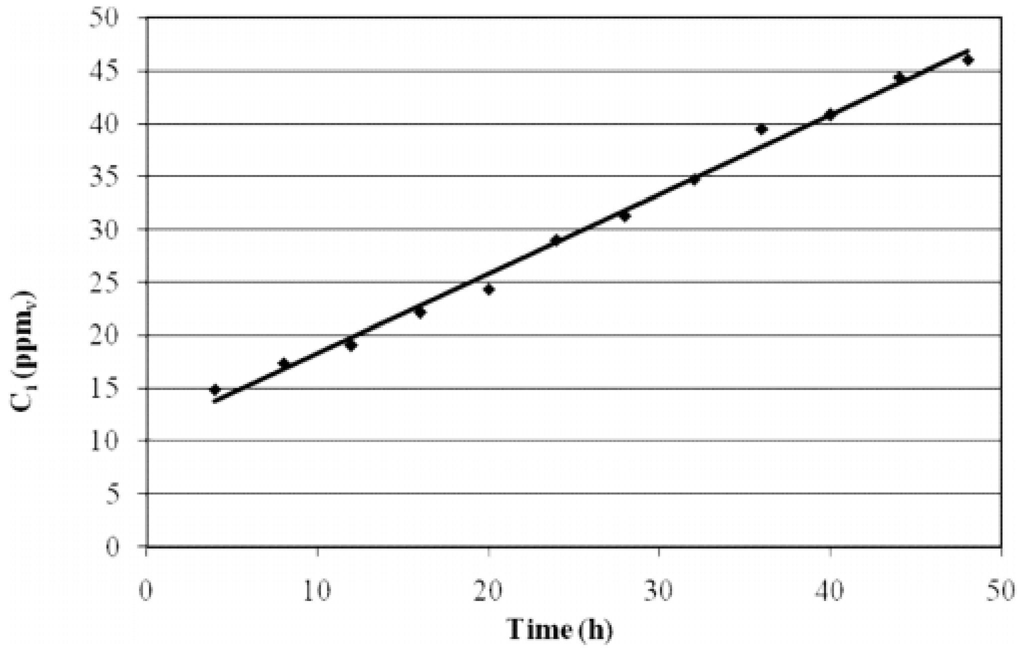

Figure 5.3 Variations of measured inlet concentrations of water vapor in natural gas with time (batch 3: Adsorption step)

- Figures 5.1, 5.2 and 5.3 show the variation of inlet concentration of water vapor in natural gas in three different batches with time, [Tables (11,12 &13) in appendix (A)]

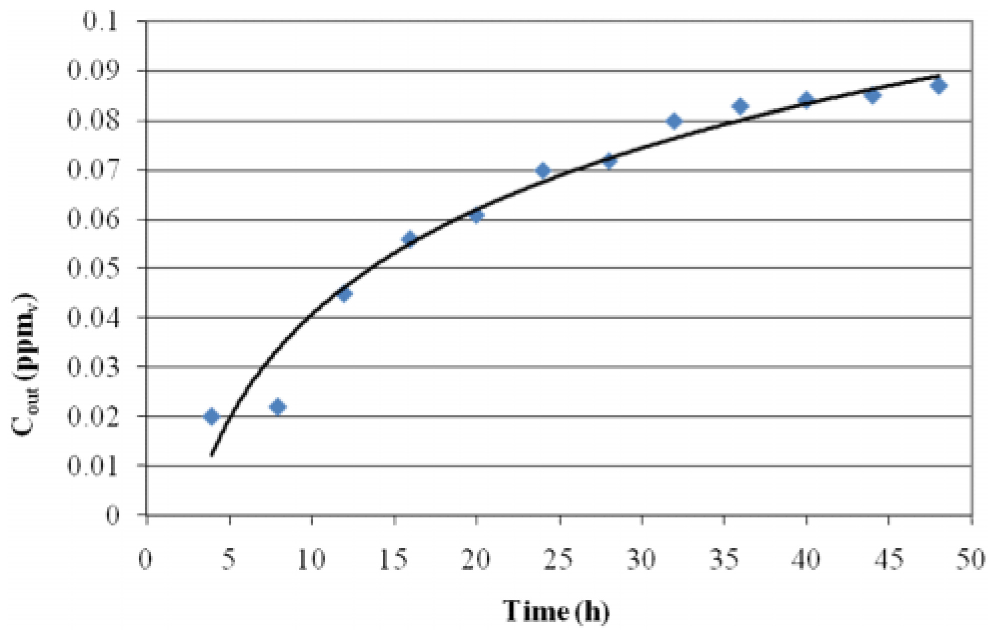

Figure 5.4 Variations of measured outlet concentrations of water vapor in natural gas with time (batch 1: Adsorption step)

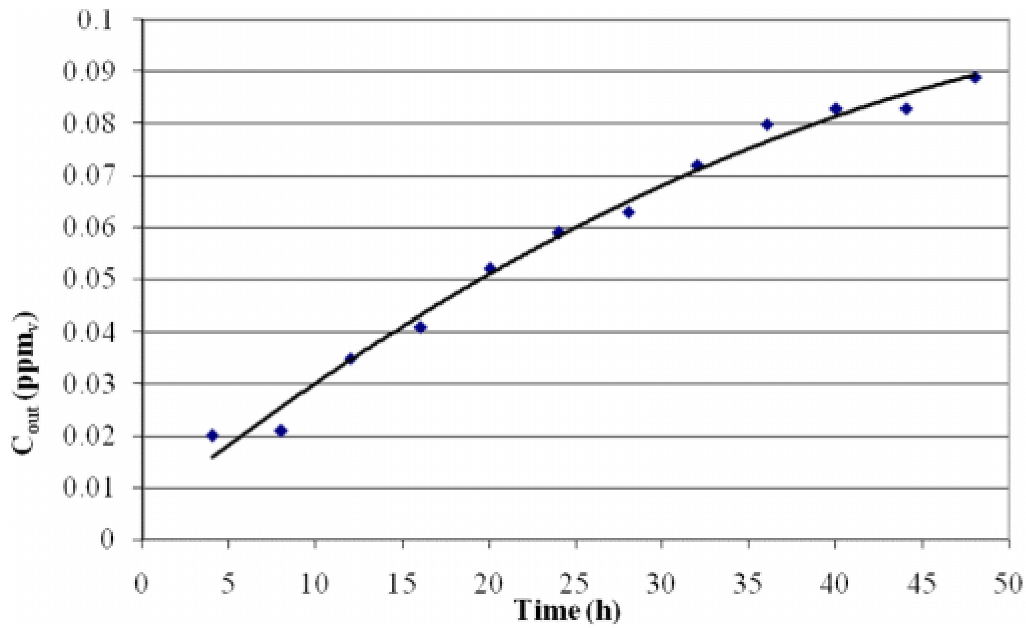

Figure 5.5 Variations of measured outlet concentrations of water vapor in natural gas with time (batch 2: Adsorption step)

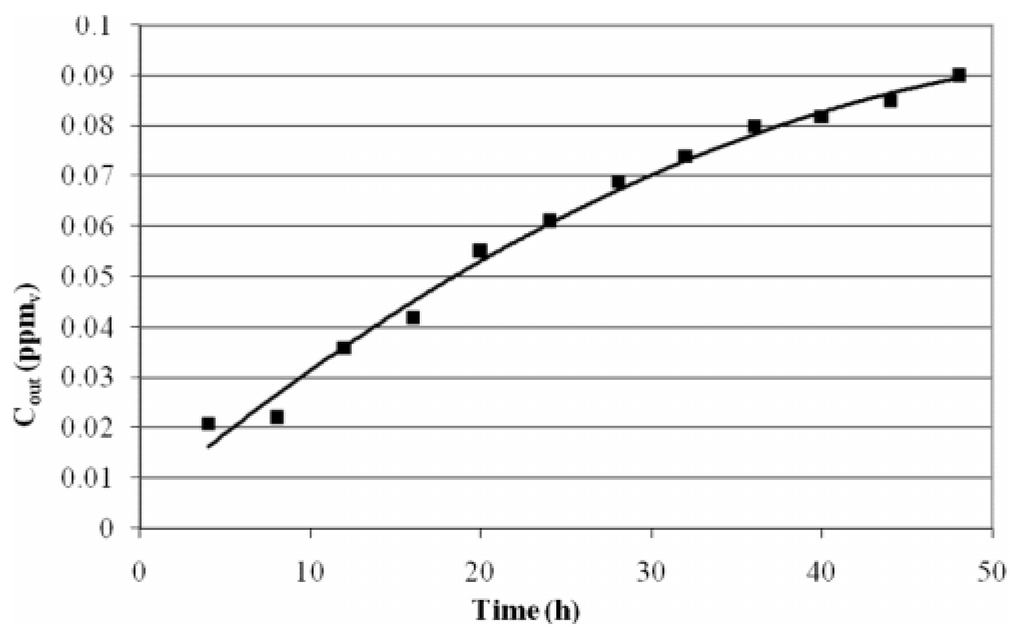

Figure 5.6 Variations of measured outlet concentrations of water vapor in natural gas with time (batch 3: Adsorption step)

- Figures 5.4, 5.5 and 5.6 show the variation of outlet concentration of water vapor in natural gas in three different batches with time, [tables (11, 12&13) in appendix (A)]. These figures show that by increasing the time the outlet concentration is increased, but the dehydration beds have not reached breakthrough zone and that is because the regeneration cycle was started after 48 hours of adsorption step according to the design criteria of unit.

❖ In all the foregoing Figures 5.1 through 5.5, one can observe the following:

1. The variation of inlet concentration with time in all batches is considerable (from 15 ppm_v to 45 ppm_v), whereas the outlet concentration variation was always limited (0.02 ppm_v to 0.086 ppm_v). This indicates the high efficiency of the molecular sieve bed for dehydration.
2. This can be due to the inlet concentration never exceeded 45 ppm_v (water vapor) while the design value was 90 ppm_v. This big margin led to such a low outlet concentration for the whole period of bed operation (about 15 **years) of 12 cycles of adsorption per month followed by regeneration.**
3. In addition to that the regeneration step was executed early and before breakthrough time as design criteria implies and to put gas plant operation in safety mode.

- **<u>Validation of the mathematical model</u>**

Table 5.1: Comparison between Estimated and Plant data

Time (h)	Plant data C_{out} (ppm_v)	Estimated C_{out} (ppm_v)	% Absolute Deviation
4	0.02	0.0203	1.5
8	0.036	0.034	5.55
12	0.051	0.048	5.89
16	0.056	0.059	5.36
20	0.064	0.068	6.25
24	0.072	0.075	4.17
28	0.079	0.08	1.27
32	0.08	0.082	2.5
36	0.083	0.084	1.2
40	0.084	0.085	1.19
44	0.085	0.086	1.17
48	0.087	0.087	0.0

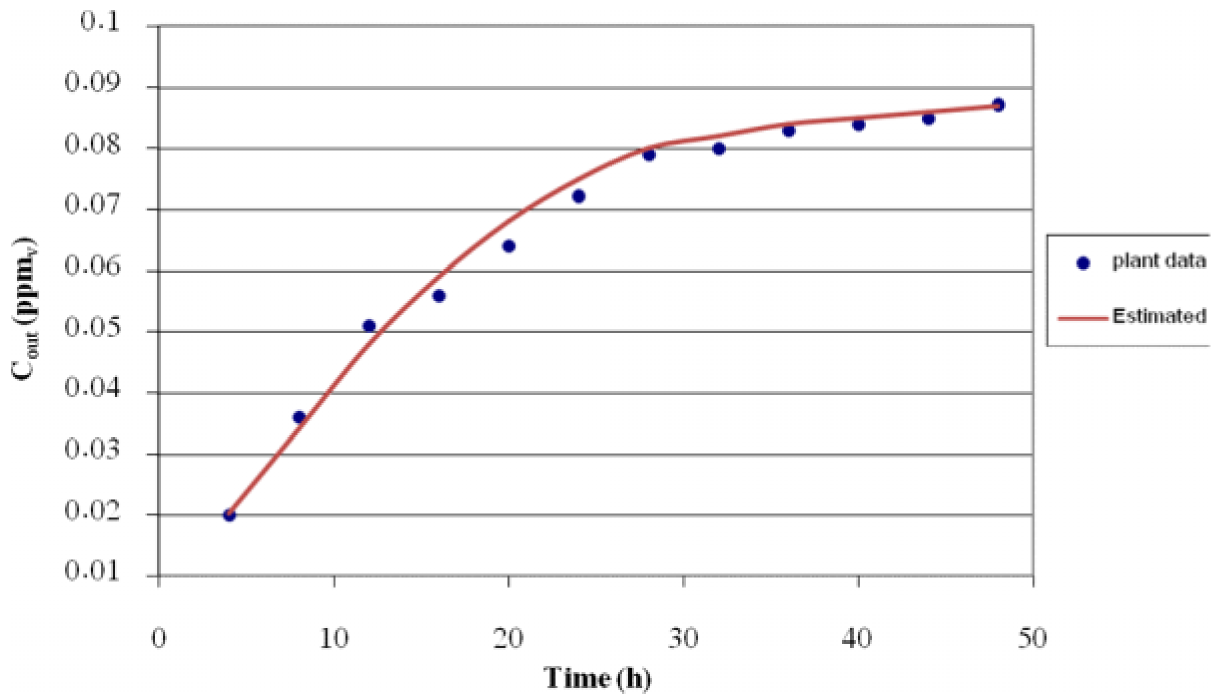

Figure 5.7 Comparison between estimated and plant data of the outlet concentration.

- Table (5.1) and figure 5.7 show the validation of the proposed model. Many trials to improve the accuracy of the data obtained as a final result by assuming different values for $\mathbf{D_p^e}$ and resolve the model to obtain a minimum value of standard error (SE). It is clear that by using value of $\mathbf{D_p^e} = 1.2\times10^{-12}$ m^2/s the developed model is very successful (SE= 3.07%) and gave results very close to actual plant data. (the range of $\mathbf{D_p^e}$ was 1×10^{-8} - 1×10^{-10} m^2/s [24])
- Fatemi, Shohreh, [19] compared the experimental results with the numerical results with standard error (SE) fluctuating between 6.6% and 7.4%. But it should be noted that the experimental data collected were for laboratory field with total sum time about 200 minutes only.
- Xi-Gang Yuan [25] developed a model which gave standard error (SE) fluctuating between 5.7% and 8.6%. Also it was applied in the laboratory field.
- Maria J. Rivero [31] compared the experimental results with the numerical results for styrene drying by adsorption onto activated alumina with standard error (SE) 7.34%.

- Sensitivity analyses of breakthrough times were applied for different flow velocities and different inlet concentration of water vapor in natural gas.

Table 5.2 Effect of natural gas velocity on Breakthrough time at an inlet water concentration of C_i = 40 ppmv

Breakthrough time (h)	2100	4100	14000	42000	54000
u_s (m/s) $\times 10^{-3}$	1.97	4.4×10^{-1}	4.49×10^{-2}	4.15×10^{-3}	4.5×10^{-4}

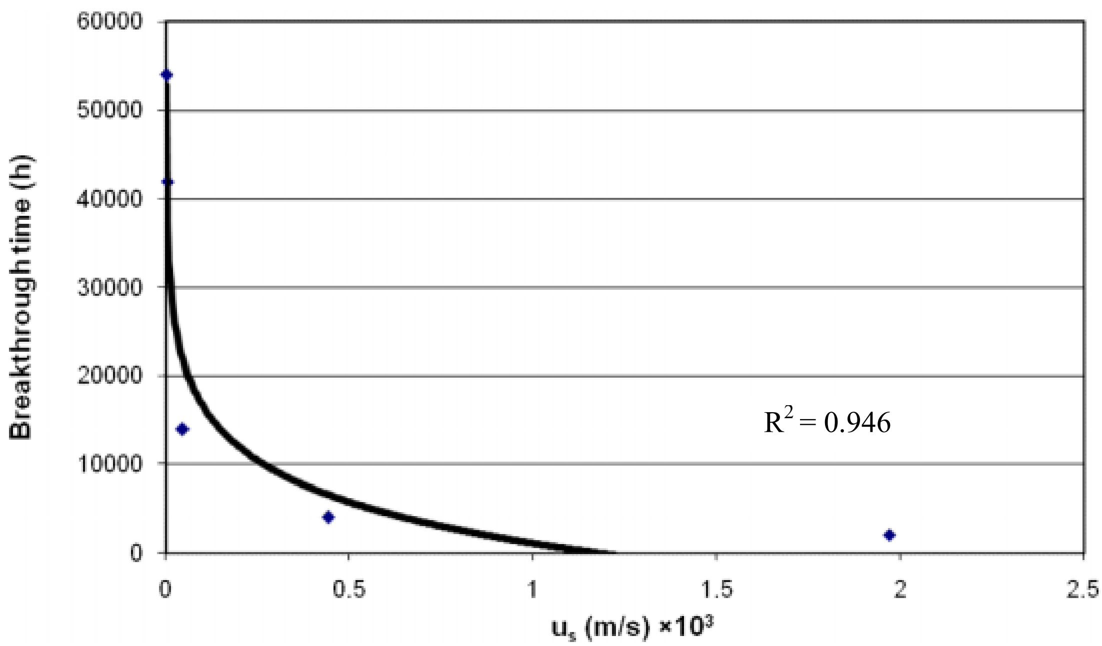

Figure 5.8 Effect of feed gas velocity on breakthrough time for gas dehydration

- Figure 5.8 shows the effect of natural feed gas velocity on Breakthrough time at an inlet water concentration of C_i = 40 ppmv.
- Notice that the breakthrough time is increased by decreasing the superficial velocity of the natural gas. That means the relationship between the superficial velocity and time is an inverse relationship.
- This figure clearly shows at low values of superficial velocity up to 4.5×10^{-7} m/s the increase in velocity has strong effect on decreasing the breakthrough time.
- The relation between feed gas superficial velocity (u_s) in m/s and breakthrough time (t_b) in hours is given by the following equation:

$$\mathbf{t_b = -\,6708\; \mathit{ln}\,(u_s) + 1187.9}$$

- From table (5.2) it's clear that at a gas velocity of 1.97×10^{-3} m/s the breakthrough was 2100 hours, the gas velocity applied in the plant is 0.2082 m/s but it is a usual practice to run the adsorption only 48 hours, there after bed regeneration takes place.

Table (5.3) Effect of inlet water vapor concentration on Breakthrough time at a superficial velocity of u_s = 0.2088 m/s

Breakthrough time (h)	560	480	300	180	160
C_i (ppmv)	40	100	200	300	400

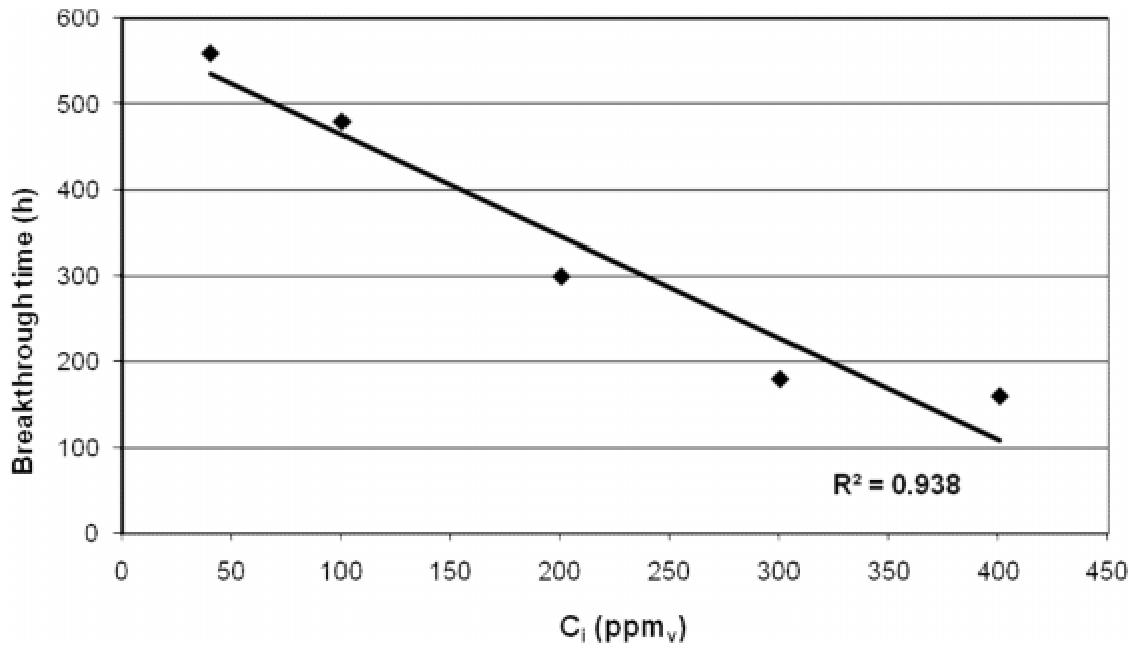

Figure 5.9 Effect of inlet concentration of feed gas on breakthrough time

- Figure 5.9 shows the effect of inlet water concentration of natural gas on Breakthrough time at a superficial velocity of u_s = 0.2088 m/s.
- It is noticed that the time decreased almost linearly by increasing the inlet concentration of water vapor. That means the relationship between the inlet concentration of water vapor and time is a reverse correlation.
- In this figure the situation is different than that of the effect of superficial velocity on breakthrough time as it shows a linear decrease of the breakthrough time with the increase in the inlet concentration of water vapor in feed gas.
- The relation between inlet concentration of water vapor (C_i) in ppm_v and breakthrough time (t_b) in hours at u_s = 0.2088 m/s is given by the following equation:

$$\mathbf{t_b = -1.1848 \times C_i + 582.44}$$

- Fatemi, Shohreh, [19] compared between two models when changing the particle radius. Also they applied the sensitivity analysis for different temperatures and inlet flow velocities. It was shown, that increasing temperature and inlet flow velocity leads to lower breakthrough time.
- Xi-Gang Yuan [25]: the model was successfully used for prediction of the breakthrough time at different superficial velocities and different bed depth, but it could not predict well the breakthrough time for different vapor concentration.

- Maria J. Rivero [31] obtained the predicted curves for different bed lengths and flow rates. A model which gave standard error (SE) fluctuating between 5.57% and 9.7% was obtained and but it was applied in the laboratory field only.

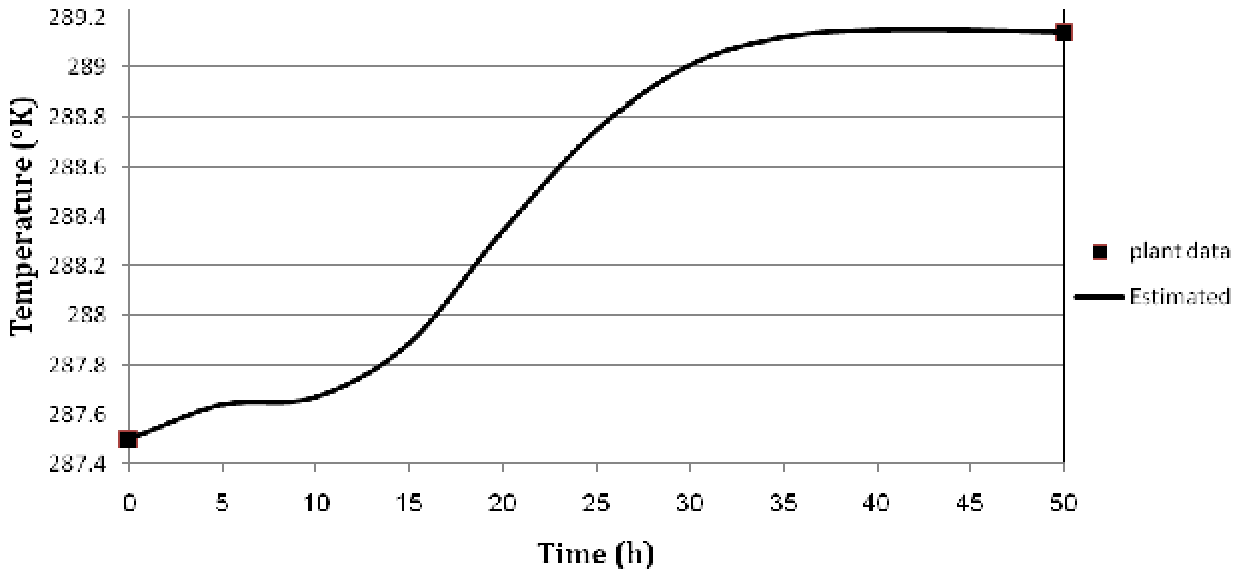

Figure 5.10: Variation of bed temperature during dehydration step (as estimated by the model) and comparison with the plant data along the bed.

- Figure 5.10 shows effect of time in the dehydration step on the temperature of gas which increased with the dehydration time increase. This is indicating that the adsorption process is exothermic and the heat effects must be considered during adsorption. The most important consideration is that the major industrial processes are adiabatic and thermal effects cannot be ignored.
- In this figure, only initial and final bed temperatures are shown from plant data.
- M. R. Talaie [17] studied the variation of gas temperature at different times.

5.1.2 Second case: separation of nitrogen by carbon molecular sieves.

Validation of the mathematical model

Table (5.4) Comparison between Estimated and Plant data

Time (hr)	Plant data N2 (mole %)	Estimated N2 (mole %)	% Deviation
0	97.9	97.9	0
3	97.9	97.8	0.102
6	97.8	97.7	0.102
9	97.6	97.6	0
12	97.6	97.7	0.102

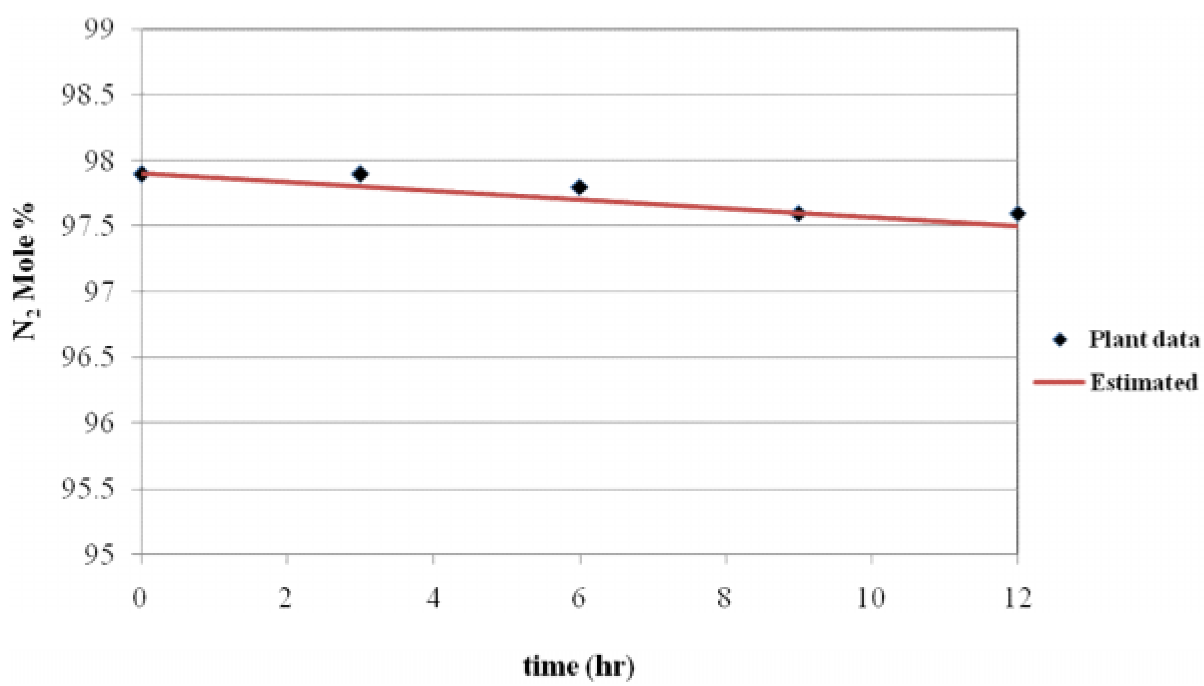

Figure 5.11 comparison between estimated and plant data of produced nitrogen mole percent

- Table 5.4 and figure 5.11 show the validation of the proposed model. Many trials were undertaken in order to improve the prediction capability of the mathematical model by assuming different values for equilibrium constant for N_2 (K) obtain a minimum value of standard error (SE). It is clear that by using value of K = 1.5 (the K value used was

2.9 [15]) the developed model is successful (SE= 2.5%) and it was validated with the plant data.

- Jafar [18] compared the estimated and experimental product purity results and found a good agreement between the model predictions and the actual data. He showed that the produced N_2 purity decreased with increasing the cycle time.
  Mostamand and Mofarahi [15] compared the experimental data for a single bed N_2 – PSA. They concluded from their simulation that the purity of N_2 decreased with the increasing time.

- Sensitivity analyses of breakthrough curves were applied for different flow velocities of air through carbon molecular sieves bed.

Table 5.5: Effect of inlet air flow velocity on purity of N_2

N_2 mol %	99.1	99.02	98.6	97.85	97.7
u_s (m/s)	0.001	0.002	0.0102	0.025	0.028

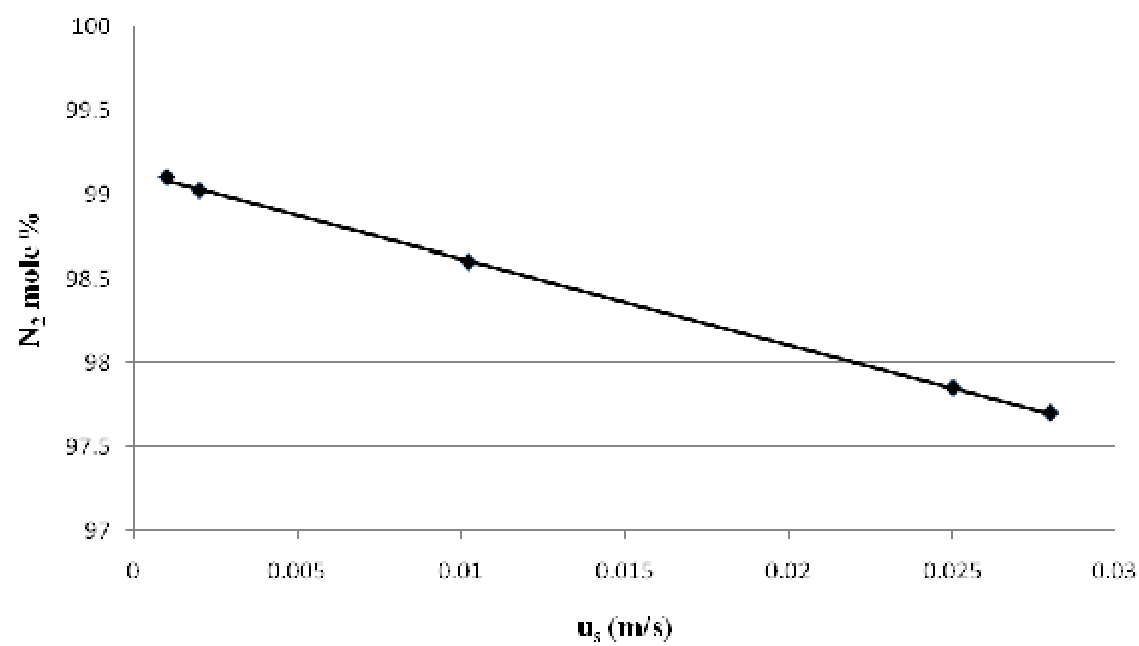

Figure 5.12 Effect of inlet air flow velocity on N_2 purity in PSA system

- Figure 5.12 shows the effect of air flow velocity on N_2 purity.
- It is noticed that the purity of N_2 produced decreased by increasing the inlet superficial velocity of the air. That means the relationship between the superficial velocity and time is a negative relationship.
- The relation between inlet air flow velocity (u_s) in m/s and N_2 mole % is shown by the following equation:

$$N_2 \text{ mole \%} = -51.35 \times u_s + 99.13$$

- Jafar [21] reported that the results show that the product of the N_2 purity increases with decreasing the inlet velocity.

5.2 CONCLUSIONS

- In the present study, a comprehensive mathematical model was developed to perform parametric study for two cases a natural gas dehydration unit and nitrogen separation by PSA located on Amerya LPG Recovery Plant of Egyptian Natural Gas Company (GASCO).
- The models in two cases were applied and a good agreement between plant data and estimated data was achieved.
- The MATLAB program was used with the system and it is currently being applied to a wide range of plant data, the program can be used for predicting the outlet concentration profile with a very large time interval.

- **In the first case (a natural gas dehydration):**
  1. By increasing the time the outlet concentration of water vapor increased because the dehydration beds will enter the saturated zone.
  2. On applying the sensitivity analysis technique by the MATLAB program, the program could clearly show the effect of varying inlet concentration of water vapor content in natural gas on breakthrough time. It was noticed that the time decreased almost linearly by increasing the inlet concentration of water vapor. Also the effect of varying natural feed gas velocity on breakthrough time was studied. It was noticed that the breakthrough time is increased by decreasing the superficial velocity of the natural gas.
  3. Effect of dehydration step on the temperature of gas and we compared the estimated data with plant data.

  It is clear that the developed model is very successful and SE= 3.07%
- I**n the second case (nitrogen separation from air by PSA)**:
  1. A model to predict the N_2 gas purity as a function of operating time of PSA unit was developed and good agreement between the plant data and estimated data with **SE= 2.5%**.
  2. By increasing the time of adsorption the purity of nitrogen producing decreased, so the system of operation stopped the adsorption cycle and enter in the regeneration cycle to maintain on the high purity of nitrogen produced.
  3. Effect of inlet air velocity on the producing of nitrogen purity and it noticed that the product of N_2 purity decreased by increasing the inlet superficial velocity of the air.

REFERENCES

1. G. McKAY, "Mass transfer processes during the Adsorption of Solutes In aqueous solutions in batch and fixed bed adsorbers", chemical engineering research & design, vol. 62, no. 4, 235-246, 1984.
2. Boyun Guo & Ali Ghalambor, "Natural Gas Engineering Handbook", Houston-Texas, Ch.1, 1-3, 2005.
3. J.M. Coulson and J.F. Richardson, "Chemical engineering" ,vol. 2, 4th edition, 1995.
4. Aitani A.M., "Sour natural gas drying", Hydrocarbon Process. Int. ed., vol. 72, no. 4, 67-73, 1993.
5. A. Karimi and MA. Abdi, "Selective Removal of Water from Supercritical Natural Gas", Society of Petroleum Engineers (SPE), 2006.
6. Babenko V. A. & Kanonchik L. E., "Mathematical modeling of a cylinder with a sorbent and natural gas", Journal of Engineering Physics and Thermo physics; vol. 73 , no 3 , 516 – 527, 2000.
7. Arthur J. Kidnay and William R. Parrish, "Fundamentals of Natural Gas Processing", Taylor & Francis group, 2,7,9-11,13,133-134,139,146-152,160-161, 2006.
8. Francis S. Manning & Richard E. Thompson, "Oilfield Processing of Petroleum", penn Well publishing company, Volume 1, Ch. 9 p. 174-177, 192-195, 1991.
9. "Engineering Data Book", 11^{st} edition, volume 2, Gas Processors Association, Ch. 20, 23, 28, 36-37, 1998.
10. D. M. Ruthven, "Principles of adsorption and adsorption process", John Wiley & sons, New York, 1984.
11. Laila Abu-Lail, John A. Bergendahi & Robert W. Thompson, “Mathematical modeling of chloroform adsorption onto fixed bed columns of highly siliceous granular zeolites”, AICHE, vol. 31, No. 4, 2012.
12. Jose A.C. Silva, "Sorption and kinetics of CO2 and CH4 in binder less beads of 13X zeolite", Microporous and Mesoporous materials, 158, 219-228, 2012.
13. Trizha L. P. Dantas, Alirio E. Rodrigues, Regina F.P.M. Moreira, "Separation of carbon dioxide from flue gas using adsorption on porous solid", Greenhouse gases – Capturing, Utilization and Reduction, 57-80, 2012.
14. Tirzha L.P. Dantas, “Carbon dioxide-nitrogen separation through adsorption on activated carbon in a fixed bed”, Chemical Engineering Journal, vol. 169, 11-19, 2011.
15. Ashkan. Mostamand & Masoud. Mofarahi, “Simulation of a single bed pressure swing adsorption for producing nitrogen”, International conference on chemical, biological and environmental science, Bangkok Dec., 2011.
16. Alirio E. Rodrigues, "Activated carbon for hydrogen purification by pressure swing adsorption multi-component breakthrough curves and PSA performance", Chemical Engineering Science, 66, 303-317, 2011.
17. M. R. Talaie, “Mathematical modeling of gas dehydration adsorption process”, Chemical Engineering Science, vol. 65, 5942-5949, 2010.
18. S. Sinha, “Modeling and Simulation for Pressure swing adsorption system for hydrogen purification”, chem. biochem. Eng. Vol.24, 409-414, 2010.
19. Fatemi, Shohreh, “Mathematical modeling of single and multi-component adsorption fixed beds to rigorously predict the mass transfer zone and breakthrough curves”, Iran J. Chem. Eng., vol. 28, No. 3, 2009.
20. Marian Simo, “Adsorption/Desorption of water and ethanol on 3A zeolite in near-adiabatic fixed bed”, Ind. Eng. Chem. Res., vol. 48, 9247-9260, 2009.

21. Jafar Sadeghzadeh Ahari, “Determination effects of process variables on nitrogen production PSA system by mathematical modeling”, petroleum & coal, vol. 50, 52-59, 2008.
22. S.M.A. Guelli U. de Souza, "Numerical study of the adsorption of dyes from textile effluents", Applied mathematical modeling, 32, 1711-1718, 2008.
23. Santosh K. Gupta, “Modeling and simulation of fixed bed adsorbers (FBAs) for multi-component gaseous separations”, Computer and Chemical Engineering, vol. 31, 1282-1295, 2007.
24. Christian Jallut, “A double linear driving force approximation for non-isothermal mass transfer modeling through bi-disperse adsorbents”, Chemical Engineering Science, vol. 62, 4040-4053, 2007.
25. Xi-Gang Yuan ,”Experiment and prediction of breakthrough curves for packed bed adsorption of water vapor on cornmeal”, Chemical Engineering and processing, vol. 45, 747-754, 2006.
26. A. Mendes, "Generalized linear driving force approximation for adsorption of multi-component mixtures", Chemical Engineering Science, 61, 3519-3531, 2006.
27. A. Karimi and MA. Abdi, "Selective Removal of Water from Supercritical Natural Gas", Society of Petroleum Engineers (SPE), 2006.
28. V. Stanciu, “separation of nitrogen from air by selective adsorption of carbon molecular sieves”, U.P.B. Sci. Bull., Series A, vol. 68, No. 2, 2006.
29. Yulong Ding, "Heat transfer of gas flow through a packed bed", Chemical Engineering Science, 61, 3532-3542, 2006.
30. Chang-Ha Lee, “Pressure swing adsorption process to purify oxygen using a carbon molecular sieve”, Chemical Engineering Science, vol. 60, 869-882, 2005.
31. Maria J. Rivero, Raquel Ibanez & M. Inmaculada Ortiz, "Mathematical modeling of styrene drying by adsorption onto activated alumina", Chemical Engineering Science, 57, 2589-2592, 2002.
32. D. Bobok and E. Besedova, "Error in the estimation of effective diffusion coefficients from sorption measurements", Slovak Society of Chemical Engineering, 54, 482-488, 2000.
33. O'Koye I.P., Benham M. and Thomas K.M., "Adsorption of gases and vapors on carbon molecular sieves", American Chemical Society", vol. 3, no. 15, 4054-4059, 1997.
34. Mohamed Arshad Sheeikh, "Adsorption equilibria and rate parameters for nitrogen and methane on maxsorb activated carbon", gas separation purification, vol. 10, no. 3, 161-168, 1996.
35. V. N. Vetokhin," Study and numerical solution of a generalized mathematical model of isothermal adsorption", Journal of Engineering Physics and Thermophysics", vol. 67, no. 5, 446-454, 1994.
36. G. Mckay, S. Mckee and H.R.J. Walters, "Solid liquid adsorption based on external mass transfer, macropore and micropore diffusion", Chemical Engineering Science, vol. 42, no. 5, 1145-1151, 1987.
37. Clive L. Dym, "Principles of mathematical modeling", Claremont, California, 2004.
38. William L. Luyben, "process modeling, simulation and control for chemical engineers, 2nd edition, McGraw-Hill Book Co, 1999.
39. Bruce E. Poling, "the properties of gases and liquids", McGraw-Hill, fifth edition, 2001.
40. Brian D. Hahn and Daniel T. Valentine," Essential MATLAB for Engineers and Scientists", third edition, Elsevier Ltd., 2007.

41. H.K. Adel-Aal and Mohamed Aggour and M.A. Fahim, "Petroleum and Gas Field Processing", New York, Ch. 12, 1-2, 2003.
42. John M. Campbell, "Gas Conditioning and Processing", Campbell petroleum series, volume 2, Ch.19, 373-389, 1984.
43. Kevin R. Coombes, Brian R. Hunt, Ronald L. Lipsman, John E. Osborn, and Garrett J.Stuck, "Differential Equations with MATLAB", John Wiley & sons. Inc., 2000.
44. Richard G. Rice and Duong D. Do, "Applied Mathematics and Modeling for Chemical Engineers", 1995.
45. Robert H. Perry & Don W. Green," Perry's Chemical Engineering Handbook", 7th edition, McGraw-Hill, Ch. 5, 48 & Ch. 16, 9,19-22, 1997.
46. A. Vinash Gupta, "Handbook of chemical engineering calculations", 3rd edition, 2004.
47. R.T. Jacobsn, E.M. Lemmon, S.G. Penoncello and Z. Shan, "Thermo-physical properties of fluid and material", ch.2, 2000.
48. www.uop.com
49. www.ScienceLab.com
50. www.EngineeringToolBox.com

APPENDICES

Appendix (A)

Batches 1,2& 3 show the different event values of C_i & C_{out} (Plant data) in three different batches for dehydration of natural gas

Table A.1: Batch (1)

Time (h)	C_i ppm$_v$	C_{out} ppm$_v$
4	15.21	0.02
8	18.06	0.036
12	20.8	0.051
16	21.9	0.056
20	27.76	0.064
24	29.02	0.072
28	31.36	0.079
32	37.21	0.08
36	38.22	0.083
40	40.84	0.084
44	41.88	0.085
48	44.84	0.087

Table A.2: Batch (2)

Time (h)	C_i ppm$_v$	C_{out} ppm$_v$
4	13.62	0.02
8	14.67	0.021
12	15.21	0.035
16	18.53	0.041
20	20.25	0.052
24	23.12	0.059
28	26.5	0.063
32	28.02	0.072
36	30.3	0.08
40	34.74	0.083
44	37.31	0.083
48	40.82	0.089

Table A.3: Batch (3)

Time (h)	C_i ppm$_v$	C_{out} ppm$_v$
4	14.92	0.021
8	17.39	0.022
12	19.04	0.036
16	22.13	0.042
20	24.38	0.055
24	29.03	0.061
28	31.34	0.069
32	34.74	0.074
36	39.51	0.08
40	40.82	0.082
44	44.44	0.085
48	45.99	0.09

Table A.4 Variation of the temperature during dehydration step and comparison with the plant data along the bed.

Time (h)	0	5	10	15	20	25	30	35	40	45	50
Estimated	287.5	287.6	287.7	287.9	288.3	288.8	289	289.1	289.2	289.2	289.1
plant data	287.5 (inlet temperature)									(outlet temperature)	289.1

Table A.5 Variables and parameters used to solve the mathematical model in this work for separation of N_2 from air on carbon molecular sieve

ρ (kg/m^3)	1.127
F (Nm^3/h)	138
Bed diam. (m)	0.5
Co (ppmv)	0.79
d_p (m)	0.025
μ (kg/ms)	0.00001902
ε_b	0.4
C_f (ppmv)	0.99
R (kg/cm^2.m^3/kmol.^{o}K)	0.0847
T (^{o}K)	313
M_{air}	29
m˙ (kg)	280
P (kg/cm^2)	7
M_{O2}	32
M_{N2}	28
$e_{1\ (O2)}$ (J)	106.7
$e_{2\ (N2)}$ (J)	71.4
$\upsilon_{1\ (O2)}$ (Ǻ)	3.467
$\upsilon_{2\ (N2)}$ (Ǻ)	3.798

	O_2	**N_2**
K1	5.82E-03	1.13E-02
K2	-7.51E-06	-2.80E-05
K3	7.94E-06	3.09E-04
K4	1381	359.7
-Δ(H) (kJ/mol)	13.81	13.39

Table A.6 Variables and parameters used to solve the mathematical model in this work for dehydration of natural gas on molecular sieve

ρ (kg/m^3)	43.4
F (m^3/h)	1608
Bed diam. (m)	2.9
C_i* (ppmv)	2.00E+05
ρ_b (kg/m^3)	700
Co (ppm_v)	30
d_p (m)	3.20E-03
μ (kg/ms)	5.90E-04
ε_b	0.3
ρ_p (kg/m^3)	2100
C_f (ppm_v)	0.09
R ($kg/cm^2.m^3/kmol.^oK$)	0.0847
T (^oK)	288
M_{gas}	19.06
$m^{\cdot}$ (kg)	9928.66
P (kg/cm^2)	50.8
M_{H2O}	18
$e_{1\ (CH4)}$ (J)	148.6
$e_{2\ (H2O)}$ (J)	809.1
$\upsilon_{1\ (CH4)}$ (Å)	3.758
$\upsilon_{2\ (H2O)}$ (Å)	2.641

Table A.7 Equilibrium Rate Parameters and Heats of adsorption of O2 and N2 for CMS [15]

	Langmuir Model		**Heat of adsorption -Δ(H) (kJ/mol)**		**Diffusion rate constants, C (s^{-1})**	
Equilibrium Constants	**O_2**	**N_2**	**O_2**	**N_2**	**O_2**	**N_2**
k1 (mol/g)	5.817×10^{-3}	1.13×10^{-2}	13.81	13.39	0.0275	0.00075
k2 (mol/g K)	-7.512×10^{-6}	-2.8×10^{-5}				
k3 (1/kPa)	7.94	30.89×10^{-5}				
k4 (K)	1381	359.7				

Table A.8 Used parameters in simulation of N2 -PSA system [21]

Feed composition	21.8% O_2, 78.2% N_2
Adsorbent	**CMS**
L(m)	1.8
R_p(m)	0.0125
E	0.4
T (^oC)	40.0
Blow down pressure (atm)	1.0 atm.
Pressurization pressure (atm)	8.0
Axial Dispersion coefficient (m^2/s)	4.876×10^{-4}
Equilibrium constant for Oxygen (KA)	9.25
Equilibrium constant for Nitrogen (KB)	8.9
LDF constant for Oxygen (kA)(s^{-1})	44.71×10^{-3}
LDF constant for Nitrogen (kB)(s^{-1})	7.62×10^{-3}
Saturation constant for Oxygen (q_{AS})(mol/m)	2.64×10^3
Saturation constant for Nitrogen (q_{BS})(mol/m)	2.64×10^3

Table A.9 Equilibrium and kinetic data and other common parameters used in the PSA simulation [15]

Adsorbent	Union Carbide molecular sieve RS-10
Feed	Dry air (79% N_2, 21% O_2)
Bed length (cm)	101.6
Bed diameter (cm)	2.08
Bed voidage	0.34
Adsorbent particle diameter (cm)	0.08
Adsorbent particle density (g/cm^3)	1.1
Saturation constant for O_2 (gmol/ cm^3)	2.1×10^{-3}
Saturation constant for N_2 (gmol/ cm^3)	2.1×10^{-3}
equilibrium constant for O_2	2.9
equilibrium constant for N_2	5.9

Appendix (B)

NAT	212 Avenue Paul Doumer 92500 Rueil MALMAISON FRANCE	Job	MOLE SIEVE
		Unit	
DESSICANT PROCESS SPECIFICATION		Location	EGYPT
		Project N°	15165
Type : 3A	Service : GAS DRYER	Data sheet N°	

REGENERATION GAS CHARACTERISTICS

		Heating	Cooling
Type		Dry gas	Dry gas
Flowrate	kg/hr	15900	15900
Pressure	kg/cm² g	51.6	51.6
Temperature	°C	260	37
Water content	mg/Nm³	0.34	0.34
Massic Cp	kcal/K.kg	0.69	0.59
Mole mass	kg/kmol	19.06	19.06
Density	kg/m³	22.3	42.8
Compressibility factor		0.99	0.89

CYCLES

Absorption :		hours	48
Regeneration :		hours	24
including :	-heating	hours	6
	-cooling	hours	3
	-stand-by	hours	15

DESSICANT

Type		Molecular sieve (type 3A)
Bulk Density	g/cm³	0.69 - 0.72
Specific Heat	kcal/kg.°C	0.23
Heat of adsorption of water	kcal/kg	1000 max
Average Crushing strenght	kg	10 - 11
Beds insulation		External
Volume	m³	21.8
Life : -expected	year	3
-guaranted	year	3
Maximal pressure drop across bed	kg/cm² g	Adsorption : 0.4 / Regeneration : 0.03

ADSORPTION COLUMNS

Number of columns		3 (2 in absorption , 1 in regeneration)
Dessicant bed diameter	mm	2900
Dessicant bed height	mm	3300

NOTES

1 . Regeneration of the dessicant is performed by the DRIED GAS available at 51.6 kg/cm² g.

2 . Cabonyl sulphide (COS) formation is minimized

TABLE 2.3 Physical Constants and Fixed Points

	Molecular Weight (g/mol)	Critical Temperature (K)	Critical Pressure (MPa)	Critical Density (kg/m³)	Triple Point (K)	Normal Boiling Point (K)	Acentric Factor	Dipole Moment (D)
Methane	16.043	190.55	4.5992	162.66	90.694	111.67	0.0114	0
Ethane	30.070	305.33	4.8718	206.58	90.352	184.55	0.0993	0
Propane	44.096	369.82	4.2471	218.50	85.480	231.06	0.1524	0.083
Butane	58.122	425.13	3.7960	227.84	134.87	272.59	0.2000	0.02
Isobutane	58.122	407.82	3.6400	224.36	113.56	261.48	0.1850	0.132
Pentane	72.149	469.70	3.3700	232.00	143.47	309.21	0.2510	0.37
Isopentane	72.149	460.35	3.3957	236.00	112.65	300.97	0.2296	0.10
Neopentane	72.151	433.75	3.1963	232.00	256.60	282.63	0.1960	0
Hexane	86.175	507.82	3.0340	233.18	177.83	341.86	0.2970	0.05
Heptane	100.20	540.13	2.7360	232.00	182.55	371.53	0.3480	
Octane	114.23	569.32	2.4970	234.90	216.37	398.77	0.3930	
Ammonia	17.030	405.40	11.333	225.00	195.50	239.82	0.2560	1.47
Argon	39.948	150.69	4.8630	535.60	83.806	87.302	−0.0022	0
Benzene	78.108	562.05	4.8940	309.00	278.70	353.23	0.2092	
Carbon dioxide	44.010	304.13	7.3773	467.60	216.59	—	0.2239	0
Carbon monoxide	28.011	132.80	3.4935	303.92	67.127	81.648	0.0510	0.10
Cyclohexane	84.161	553.64	4.0750	273.00	279.47	353.89	0.2093	0.30
Cyclopropane	42.081	398.30	5.5797	258.50	145.70	241.67	0.1305	
Deuterium	4.0282	38.340	1.6653	69.797	18.710	23.309	−0.1750	0
Ethylene	28.054	282.35	5.0418	214.24	103.99	169.38	0.0866	0
Fluorine	37.997	144.41	5.1724	592.86	53.481	85.037	0.0449	0
Heavy water	20.027	643.89	21.671	358.00	276.97	374.56	0.3640	1.90
Helium	4.0026	5.1953	0.2275	69.641	2.1768	4.2304	−0.3820	0
Hydrogen	2.0159	33.190	1.3150	30.118	13.957	20.277	0.2140	0
Hydrogen sulfide	34.082	373.60	9.1100	337.41	187.70	212.86	0.0960	0.90

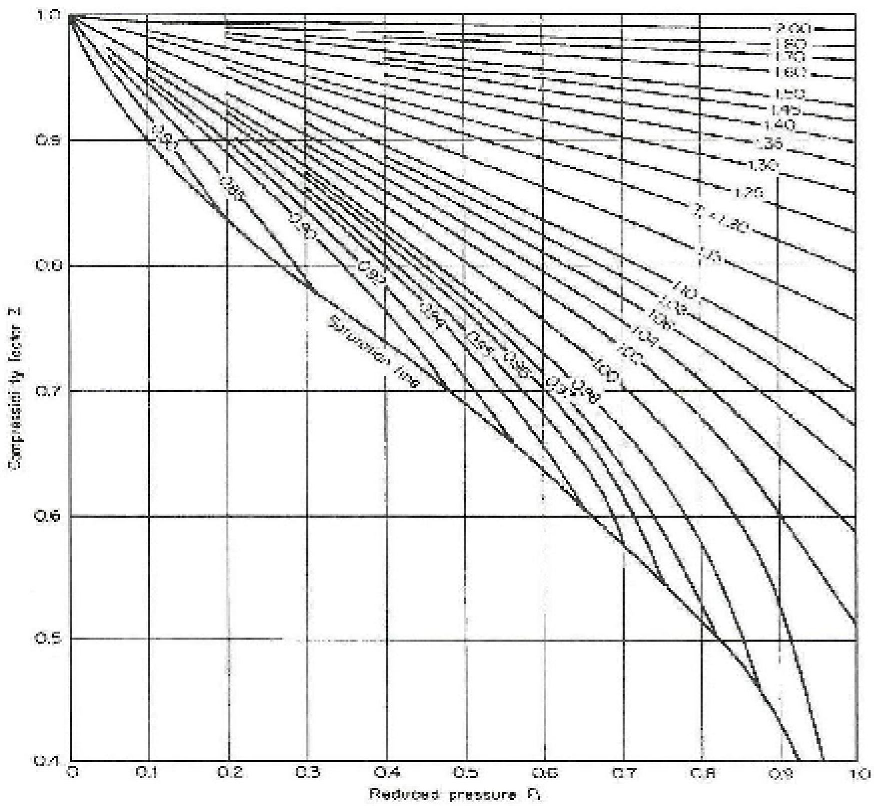

Generalized compressibility factor; $Z_c = 0.27$; low pressure range. (*Lydersen et al., University of Wisconsin Engineering Experiment Station, 1955.*)

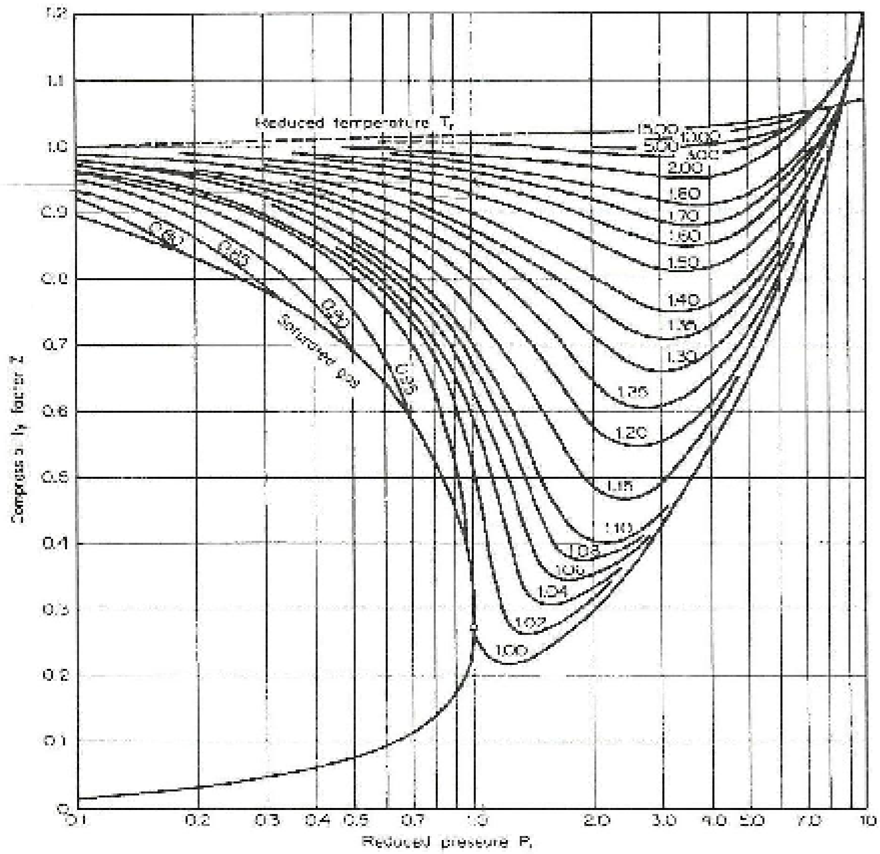

FIGURE 1.2 Generalized compressibility factor; $Z_c = 0.27$; high-pressure range. (*Lydersen et al., University of Wisconsin Engineering Experiment Station, 1955.*)

TABLE 19.1

Basic Characteristics of Molecular Sieves

Basic Type	Nominal Pore Diameter (Angstroms)	Available Form	Equilibrium H_2O Capacity (% wt)*	Molecules Adsorbed**	Molecules Excluded	Applications
3A	3	Powder 1/16-in. Pellets 1/8-in. Pellets	23 22 22	Molecules with an effective diameter <3 angstroms, including H_2O and NH_3	Molecules with an effective diameter >3 angstroms, e.g. ethane	The preferred Molecular Sieve adsorbent for the commercial dehydration of unsaturated hydrocarbon streams such as cracked gas, propylene, butadiene, and acetylene. It is also used for drying polar liquids such as methanol and ethanol.
4A	4	Powder 1/16 in. Pellets 1/8-in. Pellets 8 x 12 Beads 4 x 8 Beads 14 x 30 Mesh	28.5 22 22 22 22 22	Molecules with an effective diameter <4 angstroms, including ethanol H_2S, CO_2, SO_2, C_2H_4, C_2H_6, and C_3H_6	Molecules with an effective diameter >4 angstroms, e.g. propane	The preferred Molecular Sieve adsorbent for static dehydration in a closed gas or liquid system. It is used as a static desiccant in household refrigeration systems; in packaging of drugs, electronic components and perishable chemicals; and as a water scavenger in paint and plastic systems. Also used commercially in drying saturated hydrocarbon streams.
5A	5	Powder 1/16-in. Pellets 1/8-in. Pellets	28 21.5 21.5	Molecules with an effective diameter <5 angstroms, including $n\text{-}C_4H_9OH$**, $n\text{-}C_4H_{10}$**, C_3H_8 to $C_{22}H_{46}$, R-12	Molecules with an effective diameter >5 angstroms, e.g. iso compounds and all 4 carbon rings	Separates normal paraffins from branched-chain and cyclic hydrocarbons through a selective adsorption process.
10X	8	Powder 1/16 in. Pellets 1/8-in. Pellets	36 28 28	Iso paraffins and Olefins, C_6H_6, Molecules with an effective diameter <8 angstroms	Di-n-butylamine and larger	Aromatic hydrocarbon separation
13X	10	Powder 1/16-in. Pellets 1/8-in. Pellets	36 28.5 28.5	Molecules with an effective diameter <10 angstroms	Molecules with an effective diameter >10 angstroms, e.g. $(C_4F_9)_3N$	Used commercially for general gas drying, air plant feed purification (simultaneous removal of H_2O and CO_2) and liquid hydrocarbon and natural gas sweetening (H_2S and mercaptan removal).

Physical Properties of Adsorbents

Material and uses	Shape* of particles	Size range, U.S. standard mesh†	Internal porosity, %	Bulk dry density, kg/L	Average pore diameter, nm	Surface area, km²/kg	Sorptive capacity, kg/kg (dry)
Aluminas							
Low-porosity (fluoride sorbent)	G, S	8–14, etc.	40	0.80	~7	0.32	0.20
High-porosity (drying, separations)	G	Various	57	0.70	4–14	0.55–0.56	0.25–0.33
Desiccant, CaCl₂-coated	G	3–8, etc.	30	0.91	4.5	0.2	0.22
Activated bauxite	G	8–20, etc.	35	0.85	5		0.1–0.2
Chromatographic alumina	G, P, S	80–200, etc.	30	0.93			~0.14
Silicates and aluminosilicates							
Molecular sieves	S, C, P	Various					
Type 3A (dehydration)			~30	0.62–0.68	0.3	~0.7	0.21–0.23
Type 4A (dehydration)			~32	0.61–0.67	0.4	~0.7	0.22–0.26
Type 5A (separations)			~34	0.60–0.66	0.5	~0.7	0.21–0.22
Type 13X (purification)			~38	0.58–0.64	1.0	~0.5	0.25–0.36
Silicalite (hydrocarbons)	S, C, P	Various		0.64–0.70	0.6	~0.4	0.12–0.16
Dealuminated Y (hydrocarbons)	S, C, P	Various		0.48–0.53	0.8	0.5–0.8	0.28–0.42
Mordenite (acid drying)				0.88	0.3–0.8		0.12
Chabazite (acid drying)				0.72	0.4–0.5		0.20
LiX (air separation)	S	14–40		0.61	1.0		
Titanosilicate ETS-4 (N_2/CH_4)	S	Various	25–30	1.0	0.37		
Silica gel (drying, separations)	G, P	Various	38–48	0.70–0.82	2–5	0.6–0.8	0.35–0.50
Magnesium silicate (decolorizing)	G, P	Various	~33	~0.50		0.18–0.30	
Calcium silicate (fatty acid removal)	P		75–80	~0.20		~0.1	
Clay, acid-treated (refining of petroleum, food products)	G	4–8		0.85			
Fuller's earth (same)	G, P	<200		0.80			
Diatomaceous earth	G	Various		0.44–0.50		~0.002	
Carbons							
Shell-based	G	Various	60	0.45–0.55	2	0.8–1.6	0.40
Wood-based	G	Various	~80	0.35–0.50		0.8–1.8	0.70
Petroleum-based	G, C	Various	~80	0.45–0.55	2	0.9–1.3	0.3–0.4
Peat-based	G, C, P	Various	~55	0.30–0.50	1–4	0.8–1.6	0.5
Lignite-based	G, P	Various	70–85	0.40–0.70	3	0.6–0.7	0.3
Bituminous-coal-based	G, P	8–30, 12–40	60–80	0.40–0.60	2–4	0.9–1.2	0.4
Synthetic-polymer-based (pyrolized)	S	20–100	40–70	0.48–0.60		0.1–1.1	
Carbon molecular sieve (air separation)	C	Various	35–40	0.5–0.7	0.3–0.6		0.5–0.20
Organic polymers							
Polystyrene (removal of organics, e.g., phenol; antibiotics recovery)	S	20–60	40–50	0.64	4–20	0.3–0.7	
Polyacrylic ester (purification of pulping wastewaters; antibiotics recovery)	G, S	20–60	50–55	0.65–0.70	10–25	0.15–0.4	
Phenolic (also phenolic amine) resin (decolorizing and deashing of solutions)	G	16–50	45	0.42		0.08–0.12	0.45–0.55

*Shapes: C, cylindrical pellets; F, fibrous flakes; G, granules; P, powder; S, spheres.

†U.S. Standard sieve sizes (given in parentheses) correspond to the following diameters in millimeters: (3) 6.73, (4) 4.76, (8) 2.38, (12) 1.68, (14) 1.41, (16) 1.19, (20) 0.841, (30) 0.595, (40) 0.420, (50) 0.297, (60) 0.250, (80) 0.177, (200) 0.074.

Zeolite molecular sieve characteristics and applications

Type†	Nominal Pore Diameter Angstroms	Common Form	Bulk Density lb/cu-ft (gm/cc)	Heat of Adsorption (max) btu/lb H_2O (kcal/kg H_2O)	Equilibrium H_2O Capacity* wt-%	Molecules Adsorbed**
3A	3	Powder 1/16-inch Pellets 1/8-inch Pellets 8 x 12 Beads 4 x 8 Beads	35 (0.56) 40 (0.64) 40 (0.64) 44 (0.71) 44 (0.71)	1000 (1,000)	26 21 21 21 21	Molecules with an effective diameter <3 angstroms including H_2O and NH_3
4A	4	Power 1/16-inch Pellets 1/8-inch Pellets 8 x 12 Beads 4 x 8 Beads 14 x 30 Mesh	32 (0.51) 44 (0.71) 44 (0.71) 44 (0.71) 44 (0.71) 44 (0.71)	1800 (1,000)	27 22 22 27 22 22	Molecules with an effective diameter <4 angstroms including ethanol, H_2S, CO_2, SO_2, C_2H_4, C_2H_6 and C_3H_6
5A	5	Powder 1/16-inch Pellets 1/8-inch Pellets	32 (0.51) 44 (0.71) 44 (0.71)	1800 (1,000)	26 21.5 21.5	Molecules with an effective diameter <5 angstroms including n-C_4H_9OH, n-C_4H_{10}, C_3H_8 to $C_{22}H_{46}$, E-12
13X	8	Powder 1/16-inch Pellets 1/8-inch Pellets 8 x 12 Beads 4 x 8 Beads	27 (0.43) 40 (0.64) 40 (0.64) 40 (0.64) 40 (0.64)	1800 (1,000)	30 26 26 26 26	Molecules with an effective diameter <8 angstroms including C_6H_6, C_3H_8

†Chart depicts basic molecular sieve types only. In all applications, these basic forms are customized for specific use.
*lbs H_2O/100 lbs activated adsorbent at 17.5 torr H_2O at 25°C. **Each type adsorbs listed molecules plus those of preceding type.

TABLE 2-233 Thermodynamic Properties of Methane

Temperature K	Pressure MPa	Density mol/dm³	Volume dm³/mol	Int. energy kJ/mol	Enthalpy kJ/mol	Entropy kJ/(mol·K)	C_v kJ/(mol·K)	C_p kJ/(mol·K)	Sound speed m/s	Joule-Thomson K/MPa	Therm. cond. mW/(m·K)	Viscosity μPa·s
						Saturated Properties						
90.694	0.011696	28.142	0.035534	−1.1626	−1.1582	−0.011376	0.034773	0.054029	1539.7	−0.43891	201.94	204.93
100.00	0.034370	27.357	0.036554	−0.79798	−0.84602	−0.0080456	0.033903	0.054681	1452.0	−0.43812	210.67	155.78
105.00	0.056377	26.923	0.037143	−0.57303	−0.57097	−0.0054080	0.033590	0.055135	1403.9	−0.44908	183.03	137.80
110.00	0.088130	26.479	0.037766	−0.066592	−0.063257	−0.0018389	0.033315	0.055645	1354.7	−0.42286	156.18	121.34
115.00	0.13221	26.021	0.038431	0.15242	0.15750	0.0016441	0.032749	0.057258	1304.6	−0.40145	179.51	108.35
120.00	0.19143	25.551	0.039138	0.46455	0.47174	0.0040439	0.032409	0.055641	1253.6	−0.37589	172.16	97.462
125.00	0.26873	25.065	0.039896	0.74927	0.73999	0.0063725	0.032109	0.057741	1201.3	−0.34578	155.04	88.051
130.00	0.36732	24.562	0.040714	1.0079	1.0589	0.0086825	0.031587	0.056484	1148.1	−0.31006	157.21	79.808
135.00	0.49035	24.038	0.041600	1.3307	1.3511	0.010358	0.031469	0.059609	1093.6	−0.26735	150.75	72.629
140.00	0.64118	23.490	0.042569	1.6284	1.6557	0.012823	0.031306	0.061260	1037.7	−0.21579	142.65	66.353
145.00	0.82322	22.917	0.043636	1.9317	1.9350	0.017154	0.030874	0.062540	980.17	−0.15256	134.24	60.840
150.00	1.0400	22.309	0.044825	2.2118	2.2581	0.017264	0.030780	0.064232	920.65	−0.073012	125.40	55.437
155.00	1.2950	21.661	0.046165	2.5702	2.6159	0.019562	0.030551	0.067513	859.39	0.022798	120.32	50.652
160.00	1.5921	20.964	0.047702	2.8987	2.9647	0.021862	0.030517	0.071156	796.43	0.14606	115.19	46.236
165.00	1.9351	20.202	0.049503	3.2304	3.3265	0.023784	0.030533	0.076844	728.47	0.31398	106.11	42.135
170.00	2.3283	19.355	0.051667	3.5805	3.7008	0.025766	0.030574	0.083218	657.52	0.54097	100.75	38.117
175.00	2.7765	18.204	0.054094	3.9754	4.1744	0.028721	0.030820	0.094516	581.27	0.86918	93.384	34.136
180.00	3.2862	17.218	0.058078	4.3985	4.5873	0.030467	0.031384	0.11670	497.01	1.3868	85.789	30.132
185.00	3.8617	15.668	0.063825	4.8065	5.1480	0.033313	0.033085	0.17822	398.59	2.3397	79.044	25.170
190.00	4.5186	13.315	0.075202	5.7071	6.0658	0.038300	0.044746	1.5082	250.31	5.2409	97.958	18.947
190.56	4.5992	10.139	0.098633	6.2196	6.6077	0.041109			0	6.6877		
90.694	0.011696	0.015590	63.981	6.8816	7.5739	0.084855	0.025245	0.033851	249.13	65.621	9.8511	3.6288
100.00	0.034379	0.042978	23.262	7.0186	7.8644	0.079319	0.025427	0.034425	260.09	52.536	11.065	3.9976
105.00	0.056377	0.066175	15.113	7.1599	8.0108	0.076413	0.025695	0.034853	265.41	35.583	11.669	4.1951
110.00	0.088130	0.10025	10.035	7.2654	8.1591	0.074108	0.025946	0.035878	270.01	30.985	11.390	4.3984
115.00	0.13221	0.14457	6.9170	7.3692	8.2823	0.072026	0.026095	0.036016	274.17	25.804	12.052	4.6016
120.00	0.19143	0.20282	4.9162	7.4658	8.4067	0.070168	0.026295	0.036790	277.76	27.790	12.811	4.8175
125.00	0.26876	0.27644	3.7015	7.5559	8.5215	0.068404	0.026590	0.037771	280.76	24.838	13.641	5.0258
130.00	0.36732	0.37273	2.6825	7.6400	8.6257	0.066821	0.026854	0.038836	283.13	22.347	14.449	5.2517
135.00	0.49035	0.49962	2.0424	7.7186	8.7181	0.065121	0.027182	0.040025	284.86	20.210	15.355	5.4831
140.00	0.64118	0.62877	1.5907	7.7637	8.7970	0.064029	0.027548	0.041892	285.93	18.819	16.334	5.7254
145.00	0.82322	0.80601	1.2399	7.8405	8.8605	0.062602	0.027997	0.043092	286.31	19.780	17.436	5.9806
150.00	1.0400	1.0177	0.98256	7.8850	8.9074	0.061381	0.028432	0.046657	285.97	17.570	18.551	6.2526
155.00	1.2950	1.2724	0.78556	7.9165	8.9349	0.060028	0.028962	0.050144	284.88	17.005	19.804	6.5432
160.00	1.5921	1.5721	0.63206	7.9307	8.9560	0.058759	0.029639	0.054545	283.00	13.255	21.423	6.8688
165.00	1.9351	1.9403	0.51014	7.9233	8.9109	0.057431	0.030412	0.031406	280.30	15.600	23.225	7.2319
170.00	2.3283	2.4294	0.41163	7.8893	8.8482	0.055985	0.031379	0.071527	276.66	14.732	25.477	7.6513
175.00	2.7765	3.0428	0.32864	7.8184	8.7367	0.054371	0.032615	0.084271	271.39	13.880	28.545	8.1608
180.00	3.2862	3.8277	0.26126	7.6903	8.5480	0.052471	0.034335	0.12151	256.34	12.368	33.082	8.8251
185.00	3.8617	5.0137	0.19915	7.4515	8.2217	0.049951	0.037067	0.21701	252.37	11.482	43.707	9.9239
190.00	4.5186	7.6907	0.13016	6.7530	7.3041	0.045616	0.045765	2.2560	234.36	8.185	110.40	13.456
190.56	4.5992	10.139	0.098633	6.2196	6.6077	0.041109			0	6.6877		

Methane

Single-Phase Properties

100.00	0.10000	27.363	0.036549	−0.35363	−0.34999	−0.0038291	0.033811	0.054672	1455.6	−0.33929	199.74	153.9
111.51	0.10000	26.341	0.037963	−0.012735	−0.0090413	−0.000078677	0.033903	0.055823	1390.7	−0.41705	184.08	117.20
111.51	0.10000	0.11155	8.9655	7.2466	8.1908	0.075453	0.025304	0.035556	271.35	29.835	11.561	4.4579
200.00	0.10000	0.060615	16.594	9.8570	11.509	0.096427	0.025353	0.033784	338.36	9.2843	21.941	7.8096
300.00	0.10000	0.040139	24.931	12.175	14.665	0.10741	0.027419	0.035860	448.74	4.3218	34.532	11.245
400.00	0.10000	0.030082	33.243	15.151	18.455	0.11886	0.032500	0.040858	510.56	2.3348	50.127	14.272
500.00	0.10000	0.024055	41.572	18.673	22.82	0.12806	0.036196	0.049533	561.86	1.2245	69.564	16.876
600.00	0.10000	0.020042	49.895	22.790	27.784	0.13702	0.044179	0.052503	608.84	0.68722	88.821	19.331
100.00	1.0000	27.409	0.036483	−0.35728	−0.32179	−0.0031960	0.033850	0.054568	1459.6	−0.36660	200.82	157.61
149.14	1.0000	22.418	0.044607	2.1874	2.2325	0.015302	0.030910	0.074595	931.21	−0.085685	130.88	58.597
149.14	1.0000	0.97852	1.0220	7.5788	8.6807	0.061514	0.028253	0.045147	286.08	18.022	18.358	6.5013
200.00	1.0000	0.61383	1.5837	9.3582	10.912	0.073276	0.025872	0.035783	357.41	9.3001	23.023	8.0145
300.00	1.0000	0.40778	2.4524	12.072	14.524	0.087922	0.027821	0.036781	447.04	4.2838	35.152	11.367
400.00	1.0000	0.30205	3.3108	15.083	18.393	[illegible]	0.032361	0.041056	510.57	2.2001	50.308	14.357
500.00	1.0000	0.24058	4.1567	18.629	22.780	0.10879	0.038227	0.046766	562.99	1.1898	69.592	17.040
600.00	1.0000	0.20012	4.9971	22.733	27.732	0.11764	0.044105	0.052650	608.73	0.67124	89.293	19.455
100.00	5.0000	27.566	0.036250	−0.37098	−0.18965	−0.0038898	0.034115	0.054117	1490.0	−0.46066	204.46	165.28
200.00	5.0000	5.1706	0.19279	7.8197	8.7927	0.051895	0.032065	0.11667	291.29	6.5741	40.612	10.528
300.00	5.0000	2.1759	0.45974	11.590	13.884	0.072954	0.028602	0.041234	439.25	3.5498	39.480	12.154
400.00	5.0000	1.5[illegible]	0.65231	14.779	18.041	0.084597	0.029614	0.042307	513.11	2.0080	52.603	14.872
500.00	5.0000	1.2012	0.83249	18.402	22.583	0.094971	0.038981	0.047358	569.48	1.0870	73.309	17.418
600.00	5.0000	0.99281	1.0072	22.55	27.317	0.10427	0.044727	0.053303	618.13	0.60612	91.885	19.789
100.00	10.000	27.802	0.035969	−0.75239	0.33270	0.0071652	0.034314	0.053642	1526.7	−0.47979	209.67	174.83
200.00	10.000	16.598	0.060248	5.1777	5.7378	0.031812	0.037185	0.085065	307.02	1.0283	84.834	29.399
300.00	10.000	4.6654	0.21540	10.462	13.077	0.065137	0.029305	0.048133	441.53	2.3805	44.730	13.906
400.00	10.000	3.1042	0.32256	14.431	17.657	0.078245	0.033002	0.048223	522.58	1.7355	55.941	15.706
500.00	10.000	2.3887	0.41863	18.152	22.336	0.088665	0.038546	0.048906	580.99	0.94125	72.781	18.011
600.00	10.000	1.9659	0.50871	22.371	27.458	0.098073	0.044671	0.054070	630.63	0.51230	88.968	20.217
200.00	100.00	25.490	0.039222	9.5510	13.572	0.042590	0.032038	0.048515	1641.0	−0.30309	188.16	80.996
300.00	100.00	21.286	0.046979	7.0885	11.769	0.054186	0.031823	0.048261	1287.5	−0.44658	157.68	47.595
400.00	100.00	17.881	0.055926	11.121	16.713	0.063276	0.035275	0.050053	1115.8	−0.37694	128.99	37.264
500.00	100.00	15.005	0.066648	15.463	21.889	0.069932	0.040212	0.054129	1049.8	−0.35811	120.97	33.548
600.00	100.00	13.337	0.074979	20.074	27.581	0.076160	0.045721	0.058364	1036.9	−0.30439	130.39	32.111
200.00	500.00	33.069	0.030301	2.3895	17.492	0.0061671	0.037832	0.047321	2664.2	−0.35326	459.70	206.24
300.00	500.00	30.768	0.032482	5.9506	22.192	0.025371	0.037086	0.047111	2500.3	−0.35416	358.13	106.90
400.00	500.00	28.691	0.034567	9.7401	27.024	0.038152	0.039800	0.049943	2360.[illegible]	−0.32906	212.33	78.768
500.00	500.00	27.381	0.036686	13.804	32.228	[illegible]	0.044107	0.052486	2250.[illegible]	−0.30035	235.41	66.669
600.00	500.00	25.931	0.038559	16.815	37.802	[illegible]	0.049044	0.055917	2168.1	−0.25812	278.14	60.453

The values in these tables were generated from the NIST REFPROP software (Lemmon, E. W., McLinden, M. O., and Huber, M. L., NIST Standard Reference Database 23: Reference Fluid Thermodynamic and Transport Properties—REFPROP, National Institute of Standards and Technology, Standard Reference Data Program, Gaithersburg, Md., 2002, Version 7.1). The primary source for the thermodynamic properties is Setzmann, U., and Wagner, W., "A New Equation of State and Tables of Thermodynamic Properties for Methane Covering the Range from the Melting Line to 625 K at Pressures up to 1000 MPa," J. Phys. Chem. Ref. Data 20(6):1061–1155, 1991. The source for viscosity is Younglove, B. A., and Ely, J. F., "Thermophysical Properties of Fluids. II. Methane, Ethane, Propane, Isobutane and Normal Butane," J. Phys. Chem. Ref. Data 16:577–798, 1987. The source for thermal conductivity is Friend, D. G., Ely, J. F., and Ingham, H., "Tables for the Thermophysical Properties of Methane," NIST Tech. Note 1325, 1989.

Properties at the triple point temperature and the critical point temperature are given in the first and last entries of the saturation tables, respectively. In the single-phase table, when the temperature range for a given isobar includes a vapor-liquid phase boundary, the temperature of phase equilibrium is noted, and properties for both the saturated liquid and saturated vapor are given (with liquid properties given in the upper line). Lines are omitted from the temperature-pressure grid of the single-phase table when the system would be in the solid phase or if there are potential problems with the surface property surface.

The uncertainties in density are 0.03% for pressures below 12 MPa and temperatures below 353 K and up to 0.07% for pressures less than 50 MPa. For the speed of sound, the uncertainty ranges from 0.03% in the vapor phase to 0.3% depending on temperature and pressure. Heat capacities may be generally calculated within an uncertainty of 1%. The uncertainty in viscosity is 2% except in the critical region which is 5%. The uncertainty in thermal conductivity of the dilute gas between 130 and 625 K is 2.5%. For temperatures below 130 K, the uncertainty is less than 1%. Excluding the dilute gas, the uncertainty is 2% between 110 and 725 K at pressures up to 70 MPa, except near the critical point which has an uncertainty of 5% or greater. For the vapor at lower temperatures and the dense liquid near the triple point, an uncertainty of 10% is possible.

Thermodynamic Properties of Nitrogen (Concluded)

Temperature K	Pressure MPa	Density mol/dm³	Volume dm³/mol	Int. energy kJ/mol	Enthalpy kJ/mol	Entropy J/(mol·K)	C_v J/(mol·K)	C_p J/(mol·K)	Sound speed m/s	Joule-Thomson K/MPa	Therm. cond. mW/(m·K)	Viscosity μPa·s
						Saturated Properties						
100.00	1.3886	2.0616	0.48511	1.7573	2.4183	0.12557	0.025750	0.055392	181.18	15.070	14.410	5.1867
111.00	1.5520	2.3830	0.41912	1.7377	2.3561	0.13131	0.026054	0.061525	180.28	14.640	14.564	5.7716
113.00	1.7271	2.7243	0.36706	1.7102	2.3178	0.13250	0.026284	0.067435	179.15	13.886	15.315	6.3580
115.00	1.8870	3.1152	0.32091	1.6729	2.2440	0.13255	0.027721	0.077019	177.75	13.409	16.580	6.4332
117.00	2.1593	3.5733	0.27944	1.6234	2.2251	0.13138	0.028723	0.090166	176.01	12.767	18.186	6.8472
119.00	2.3868	4.1373	0.24172	1.5573	2.1511	0.13008	0.029037	0.11322	173.87	12.645	21.328	10.336
121.00	2.6361	4.9330	0.20670	1.4665	2.0115	0.13360	0.031583	0.15263	171.17	11.909	23.424	10.965
123.00	2.9118	5.7940	0.17287	1.3349	1.8576	0.13077	0.034185	0.21420	167.46	10.148	24.694	11.813
125.00	3.2050	7.3244	0.13653	1.1088	1.6417	0.12400	0.039579	0.69712	160.26	6.0030	41.535	13.396
126.19	3.3958	11.184	0.089414	0.51527	0.81491	0.11607			0	6.0831		
						Single-Phase Properties						
100.00	0.10000	0.12268	8.1514	2.0386	2.8547	0.13850	0.021040	0.030022	201.63	16.093	9.3807	6.9581
800.00	0.10000	0.0150347	66.508	2.571	17.561	0.2121	0.021788	0.030178	490.37	0.021463	44.5	29.577
1100.0	0.10000	0.010930	91.480	24.25	33.133	0.23101	0.024332	0.032748	580.05	−0.07954	70.073	34.76
1900.0	0.10000	0.0063156	158.30	37.872	50.879	0.24416	0.026815	0.035130	785.94	−0.81545	92.3	58.766
100.00	1.0000	24.658	0.040554	−3.1007	−2.0501	0.069143	0.027545	0.058458	663.2	−0.04514	106.8	73.255
103.75	1.0000	23.768	0.042073	−1.5441	−1.5023	0.058028	0.027281	0.058113	554.29	0.15098	98.733	67.782
103.75	1.0000	1.4754	0.67778	1.7601	2.1577	0.11766	0.023452	0.046272	182.78	15.471	11.071	7.8351
800.00	1.0000	0.15000	6.6649	17.554	17.592	0.19030	0.021812	0.030036	498.52	0.001465	44.832	29.629
1100.0	1.0000	0.10926	9.1525	24.277	33.459	0.21120	0.024318	0.032967	582.07	−0.33840	70.155	44.521
1900.0	1.0000	0.063383	15.775	37.270	50.956	0.22520	0.025820	0.035138	750.64	−0.51812	92.388	58.11
100.00	5.0000	25.496	0.039222	−3.2146	−2.0100	0.066199	0.027713	0.059808	373.34	−0.17088	108.59	84.510
600.00	5.0000	0.99608	1.0105	13.400	17.667	0.17048	0.021551	0.030325	509.60	−0.027373	45.797	26.952
1100.0	5.0000	0.53767	1.8599	24.245	33.541	0.18953	0.024349	0.033536	571.68	−0.67112	70.836	44.338
1600.0	5.0000	0.37345	2.6821	37.258	50.721	0.2110	0.025809	0.035170	798.15	−0.57585	95.665	58.478
100.00	10.000	26.135	0.038263	−2.3365	−1.9580	0.061962	0.028001	0.050446	731.22	−0.25055	115.80	95.068
800.00	10.000	1.0152	0.92075	12.389	17.581	0.17455	0.021865	0.030826	526.87	−0.12856	48.885	30.584
1100.0	10.000	1.0546	0.94453	24.211	33.654	0.19298	0.025808	0.032447	682.37	−0.38384	71.173	44.495
1300.0	10.000	0.74495	1.3616	37.245	50.864	0.20683	0.026863	0.035200	907.57	−0.82170	93.033	58.579
600.00	500.00	27.445	0.036461	18.798	29.003	0.13791	0.026406	0.034318	1574.4	−0.70223	177.40	103.10
1100.0	500.00	21.868	0.045729	21.840	48.705	0.15915	0.027986	0.035818	1701.4	−0.72340	149.37	74.801
1600.0	500.00	19.335	0.051511	37.584	94.855	0.17283	0.029647	0.036665	1603.8	−0.73758	144.17	74.926
600.00	1000.0	34.270	0.024180	1.714	40.846	0.13763	0.029193	0.036906	2107.2	−0.81888	273.07	205.33
1100.0	1000.0	30.398	0.032897	37.965	59.122	0.15332	0.029572	0.038577	1865.1	−0.38271	242.18	129.86
1600.0	1000.0	26.920	0.035380	38.488	77.570	0.16782	0.029477	0.037215	1848.9	−0.38159	214.94	116.53

The values in these tables were generated from the NIST REFPROP software (Lemmon, E. W., McLinden, M. O., and Huber, M. L., NIST Standard Reference Database 23: Reference Fluid Thermodynamic and Transport Properties—REFPROP, National Institute of Standards and Technology, Standard Reference Data Program, Gaithersburg, MD, 2002, Version 7.0). The primary source for the thermodynamic properties is Span, R., Lemmon, E. W., Jacobsen, R. T., Wagner, W., and Yokozeki, A., "A Reference Quality Thermodynamic Property Formulation for Nitrogen," *J. Phys. Chem. Ref. Data* 29(6):1361–1433, 2000. See also *Int. J. Thermophys.* 14(4):1121–1132, 1998. The source for viscosity is Lemmon, E. W., and Jacobsen, R. T., "Viscosity and Thermal Conductivity Equations for Nitrogen, Oxygen, Argon, and Air," *Int. J. Thermophys.* 25:21–69, 2004. The source for thermal conductivity is Lemmon, E. W., and Jacobsen, R. T., "Viscosity and Thermal Conductivity Equations for Nitrogen, Oxygen, Argon, and Air," *Int. J. Thermophys.* 25:21–69, 2004.

Properties at the triple point temperature and the critical point temperature are given in the first and last entries of the saturation tables, respectively. In the single-phase table, when the temperature range for a given isobar includes a vapor-liquid phase boundary, the temperature of phase equilibrium is noted, and properties for both the saturated liquid and saturated vapor are given (with liquid properties given in the upper line). Lines are omitted from the temperature-pressure grid of the single-phase table when the system would be in the solid phase or if there are potential problems with the source property surface.

The uncertainty in density of the equation of state is 0.02% from the triple point up to temperatures of 523 K and pressures up to 12 MPa and from temperatures of 240 to 523 K at pressures less than 30 MPa. In the range from 270 to 350 K at pressures less than 12 MPa, the uncertainty in density is 0.01%. The uncertainty at very high pressures (>1 GPa) is 0.6% in density. The uncertainty in pressure in the critical region is estimated to be 0.02%. In the gaseous and supercritical region, the speed of sound can be calculated with a typical uncertainty of 0.005 to 0.1%. At liquid states and at high pressures, the uncertainty increases to 0.5% to 1.5%. For pressures up to 30 MPa, the estimated uncertainty for heat capacities ranges from 0.3% at gaseous and gaslike supercritical states up to 0.8% at liquid states and at certain gaseous and supercritical states at low temperatures. The uncertainty is 2% for pressures up to 200 MPa and larger at higher pressures. The estimated uncertainties of vapor pressure, saturated liquid density, and saturated vapor density are in general 0.02% for each property. The formulation yields a reasonable extrapolation behavior up to the limits of chemical stability of nitrogen.

For viscosity, the uncertainty is 0.5% in the dilute gas. Away from the dilute gas (pressures greater than 1 MPa and in the liquid), the uncertainties are as low as 1% between 270 and 300 K at pressures less than 100 MPa, and increase outside that range. The uncertainties are around 2% at temperatures of 180 K and higher. Below this and away from the critical region, the uncertainties steadily increase to around 5% at the triple points of the fluids. The uncertainties in the critical region are higher.

For thermal conductivity, the uncertainty for the dilute gas is 2% with increasing uncertainties near the triple point. For the non-dilute gas, the uncertainty is 2% for temperatures greater than 150 K. The uncertainty is 3% at temperatures less than the critical point and 5% in the critical region, except for states very near the critical point.

The Engineering ToolBox

Home www.EngineeringToolBox.com

Resources, Tools and Basic Information for Engineering and Design of Technical Applications!

Search

Google™ Custom Search

Air Properties

Temperature, density, specific heat, thermal conductivity, expansion coefficient, kinematic viscosity and Prandtl's number for temperatures ranging *-150 - 400°C*

Common properties for air at atmospheric pressure are indicated the table below

Temperature - *t* - (°C)	Density - - (kg/m^3)	Specific heat capacity - c_p - (kJ/kg.K)	Thermal conductivity - *l* - (W/m.K)	Kinematic viscosity - *v* - x 10^{-6} (m^2/s)	Expansion coefficient - *b* - x 10^{-3} (1/K)	Prandtl's number - P_r -
-150	2.793	1.026	0.0116	3.08	8.21	0.76
-100	1.980	1.009	0.0160	5.95	5.82	0.74
-50	1.534	1.005	0.0204	9.55	4.51	0.725
0	1.293	1.005	0.0243	13.30	3.67	0.715
20	1.205	1.005	0.0257	15.11	3.43	0.713
40	1.127	1.005	0.0271	16.97	3.20	0.711
60	1.067	1.009	0.0285	18.90	3.00	0.709

ملخص الرسالة

- مما لا شك فيه أن استخدام الحاسب الآلي في مجال معالجة الغاز الطبيعي أمر ضروري لتوفير الكثير من الجهد والمال معاً. وقد ساعد تداول النماذج الرياضية لإجراء الأبحاث المختلفة لتحسين أداء وحدات المعالجة المختلفة.

- تناول هذا البحث عمل اختبار وتطوير لنموذج رياضي باستخدام برنامج كمبيوتر لحالتين تم دراستهم. إحداهما وحدة تجفيف الغاز الطبيعي باستخدام المناخل الجزيئية والتوقع بتركيز المحتوي المائي للغاز الطبيعي بعد خروجه من وحدة التجفيف وكذلك التوزيع الحراري داخل جهاز التجفيف. والثانية وحدة توليد النيتروجين من الهواء باستخدام المناخل الجزيئية الكربونية وقد تم دراسة تأثير تغيير سرعات هواء التغذية علي نقاوة النيتروجين المنتج باستخدام الامتزاز بالضغط المتأرجح (pressure swing adsorption) .
- النموذج الرياضي الاول يعتمد علي المعادلات التفاضلية الجزيئية للموازنة المادية والحرارية مع وضع بعض الافتراضات حتي تستخدم لحل هذه المعادلات. والنموذج الثاني لإنتاج النيتروجين وقد تم تطبيق الموازنة المادية.

- كما تم تطبيق تقنية تحليل الحساسية (Sensitivity analysis) لمعرفة مدي دقة النموذج ومدي تطبيقه علي وحدات تجفيف الغاز الطبيعي باستخدام المناخل الجزيئية ووحدة توليد النيتروجين من الهواء باستخدام المناخل الجزيئية الكربونية وذلك باستخدام تركيزات مختلفة للمحتوي المائي لغازات التغذية وكذلك مع تغيير سرعات غازات التغذية المارة من خلال وحدة تجفيف الغاز الطبيعي نظرياً و تم الوصول الي علاقات رياضية لتلك التأثيرات، كما تم التوصل الي علاقة رياضية لمعرفة مدي تأثير تغيير سرعات الهواء المغذية لوحدة توليد النيتروجين علي نقاوة النيتروجين المنتج.
- تم اختبار النموذج الرياضي وتم تطويره ليتطابق مع وحدة تجفيف الغاز الطبيعي باستخدام المناخل الجزيئية ووحدة توليد النيتروجين من الهواء باستخدام المناخل الجزيئية الكربونية المستخدمة بمصنع استخلاص البوتاجاز بالعامرية التابع للشركة المصرية للغازات الطبيعية وقد تم عمل برنامج مساعدة علي الحاسب الآلي لحل النموذج الرياضي باستخدام Matlab.

- كما تناول البحث جزءاً نظرياً شارحاً فيه الطرق المختلفة لعملية التجفيف و الامتزاز بالضغط المتأرجح.

جامعة الإسكندرية
كلية الهندسة
الهندسة الكيميائية

تطوير نموذج رياضي لتجفيف الغاز الطبيعي وإنتاج غاز النيتروجين النقي

رسالة علمية

مقدمة إلى الدراسات العليا بكلية الهندسة – جامعه الإسكندرية

استيفاء للدراسات المقررة للحصول على درجة الدكتوراه

مقدمه من

مهندس / محمد السيد أحمد جاد

فبراير 2015